Computational study on the affinity of potential drugs to SARS-CoV-2 main protease

IOP Publishing Journal of Physics: Condensed Matter
J. Phys.: Condens. Matter **34** (2022) 294005 (13pp) https://doi.org/10.1088/1361-648X/ac6c6c

Computational study on the affinity of potential drugs to SARS-CoV-2 main protease

Verónica Martín[1], Miguel Sanz-Novo[1,2], Iker León[1,2], Pilar Redondo[1], Antonio Largo[1,*] and Carmen Barrientos[1]

[1] Departamento de Química Física y Química Inorgánica, Universidad de Valladolid, 47011 Valladolid, Spain
[2] Grupo de Espectroscopía Molecular (GEM), Edificio Quifima, Área de Química-Física, Laboratorios de Espectroscopía y Bioespectroscopía, Parque Científico UVa, Unidad Asociada CSIC, Universidad de Valladolid, 47011 Valladolid, Spain

E-mail: antonio.largo@uva.es

Received 30 January 2022, revised 22 April 2022
Accepted for publication 3 May 2022
Published 18 May 2022

Abstract

Herein, we report a computational investigation of the binding affinity of dexamethasone, betamethasone, chloroquine and hydroxychloroquine to SARS-CoV-2 main protease using molecular and quantum mechanics as well as molecular docking methodologies. We aim to provide information on the anti-COVID-19 mechanism of the abovementioned potential drugs against SARS-CoV-2 coronavirus. Hence, the 6w63 structure of the SARS-CoV-2 main protease was selected as potential target site for the docking analysis. The study includes an initial conformational analysis of dexamethasone, betamethasone, chloroquine and hydroxychloroquine. For the most stable conformers, a spectroscopic analysis has been carried out. In addition, global and local reactivity indexes have been calculated to predict the chemical reactivity of these molecules. The molecular docking results indicate that dexamethasone and betamethasone have a higher affinity than chloroquine and hydroxychloroquine for their theoretical 6w63 target. Additionally, dexamethasone and betamethasone show a hydrogen bond with the His41 residue of the 6w63 protein, while the interaction between chloroquine and hydroxychloroquine with this amino acid is weak. Thus, we confirm the importance of His41 amino acid as a target to inhibit the SARS-CoV-2 Mpro activity.

Keywords: molecular docking, dexamethasone, betamethasone, chloroquine, hydroxychloroquine, SARS-CoV-2 main protease

S Supplementary material for this article is available online

(Some figures may appear in colour only in the online journal)

1. Introduction

Severe acute respiratory syndrome coronavirus 2, SARS-CoV-2, is a human coronavirus type that emerged in late 2019 and has caused the coronavirus disease, or COVID-19 global pandemic. This affliction is airborne, and is transmitted by inhaling suspended droplets or aerosols exhaled by an infected person [1]. The structure of the SARS-CoV-2 consists of a single-stranded RNA located inside a lipid membrane [2]. Coronaviruses contain a genome composed of a long RNA strand that acts as a messenger RNA when it infects a cell. It addresses the synthesis of two long polyproteins, pp1a

* Author to whom any correspondence should be addressed.

and pp1ab, which provide the machinery the virus needs to replicate new viruses [3]. These polyproteins have a replication/transcription complex that produces more RNA, several structural proteins that construct new virions, and two proteases. The latest play an essential role in cleaving the polyproteins into all of these functional parts.

In current pharmaceutical research, one of the strategies to address the COVID-19 is the design of drugs able to inhibit the activity of the SARS-CoV-2 proteases. The main protease of the virus, Mpro, also known as 3C-like protease 3CLpro, is a key enzyme for the viral replication and transcription process. Mpro digests the polyprotein at least eleven conserved sites, starting with the autolytic cleavage of this enzyme itself from pp1a and pp1ab [4]. The functional importance of Mpro in the viral life cycle makes this protease an attractive target for the design of antiviral drugs. In addition, this protease is not found in humans, so if it is specifically attacked, there is little chance of side effects.

Mpro, formally known as C30 endopeptidase, is a cysteine protease exhibiting high specificity to induce selective cleavage of the peptide bonds and infect cells. It is made of three domains, finding the active center laying at their core. Mpro has a cysteine–histidine catalytic dyad at its active site and cleaves a Gln–(Ser/Ala/Gly) peptide bond. Thus, it was proposed histidine 41 (His41) and cysteine 145 (Cys145) [5] as the most relevant amino acids to inhibit the SARS-CoV-2 Mpro activity.

Within this framework, one of the non-antiviral drugs that has shown a positive effect for treating COVID-19 patients is dexamethasone. This drug was recommended for COVID-19 patients who need either mechanical ventilation or supplemental oxygen by the National Health Service in the UK and the National Institutes of Health in the US [3].

Dexamethasone ($C_{22}H_{29}FO_{25}$) is a synthetic fluorinated corticosteroid derived from prednisolone, to which a fluorinated radical has been introduced, and whose chemical formula is 9α-fluoro-11β,17α,21-trihydroxy-16α,-methylpregna-1,4-diene-3,20-dione. It consists of twenty-one carbon atoms arranged in four rings. Dexamethasone was initially developed as a glucocorticoid receptor-specific agonist [6]. Its enantiomeric form, betamethasone, is also a potent corticosteroid that is widely used in the treatment of inflammation, allergies and other important treatments, such as to prevent transplant patients from rejecting the new organ [7]. In figure 1, we show the 2D structures of dexamethasone and betamethasone.

Recent researches [8, 9] on the use of dexamethasone in the treatment of COVID-19 propose a mechanism of action, in which the interaction between the centroid of the pregnanous ring with the sulfur atom of cysteine 145 (Cys145) occurs. Additionally, dexamethasone interacts with glycine 143 (Gly143) through the carbonylic oxygen via a hydrogen bond. This interaction could be strong enough to inhibit protease activity; thus, hampering the action of the virus on the human body.

Similarly, dexamethasone, chloroquine ($C_{18}H_{26}ClN_3$) and hydroxychloroquine ($C_{18}H_{26}ClN_3O$) (see figure 1), two drugs that are commonly used to prevent and treat malaria, were also studied to treat COVID-19. Chloroquine (4-N-(7-chloroquinolin-4-yl)-1-N,1-N-diethylpentane-1,4-diamine) is an aminoquinoline used for the prevention and therapy of malaria. It is also effective in extraintestinal amebiasis and as an antiinflammatory agent for therapy of rheumatoid arthritis and lupus erythematosus. Hydroxychloroquine (2-[4-[(7-chloroquinolin-4-yl)amino]pentyl-ethylamino]ethanol) is a derivative of chloroquine in which one of the N-ethyl groups is hydroxylated at position 2. It is a commonly prescribed medication in the treatment of uncomplicated malaria, rheumatoid arthritis, chronic discoid lupus erythematosus, and systemic lupus erythematosus. Moreover, hydroxychloroquine is also used for the prophylaxis of malaria in regions where chloroquine resistance is unlikely.

Chloroquine and hydroxychloroquine were both investigated for the treatment of SARS-CoV-2. However, most studies were halted early in the pandemic mainly due to two reasons [10, 11]: on the one hand, it was concluded that these drugs have little or no effect on the risk of death and probably no effect on progression to mechanical ventilation, and, therefore, they are not effective in treating COVID-19 or its exacerbation; on the other hand, they may increase the risk of adverse events.

Nevertheless, even with effective vaccines available, functional drugs are currently needed to treat infected people. In this context, a rational drug design can reduce significantly the time needed in the drug discovery process. Thus, molecular docking can be employed to identify lead molecules against the target proteins.

Molecular docking is a powerful and efficient method for structure-based drug discovery by testing whether existing antiviral molecules can effectively treat associated viral infections [12]. This procedure predicts the intermolecular framework formed between a protein and a small molecule (ligand) and shows the binding modes responsible for inhibition of the protein [13].

In the last few years several researches have been devoted to find efficient inhibitors against SARS-CoV-2 main protease using computational methods [14–20]. In the present work, we report a theoretical study using molecular and quantum mechanics methodologies on the molecular structure and antiviral activity of dexamethasone, betamethasone, chloroquine and hydroxychloroquine in the treatment of COVID-19. We chose dexamethasone and betamethasone as reference drugs that have shown promising results in the treatment of COVID-19, while we selected chloroquine and hydroxychloroquine as reference drugs where no benefit was observed in patients with mild COVID-19 [21]. This study primarily involves a conformational analysis of the dexamethasone, betamethasone, chloroquine and hydroxychloroquine molecules. Subsequently, we carried out a spectroscopic analysis and a study of the molecular orbitals for the most stable conformers. We determined the reactivity indices, which enable predicting the chemical reactivity of the molecules. The reactivity indices also allow us to find the sites of the nucleophilic and electrophilic regions of the molecules. Finally, we employed the optimized structures of ligands to perform

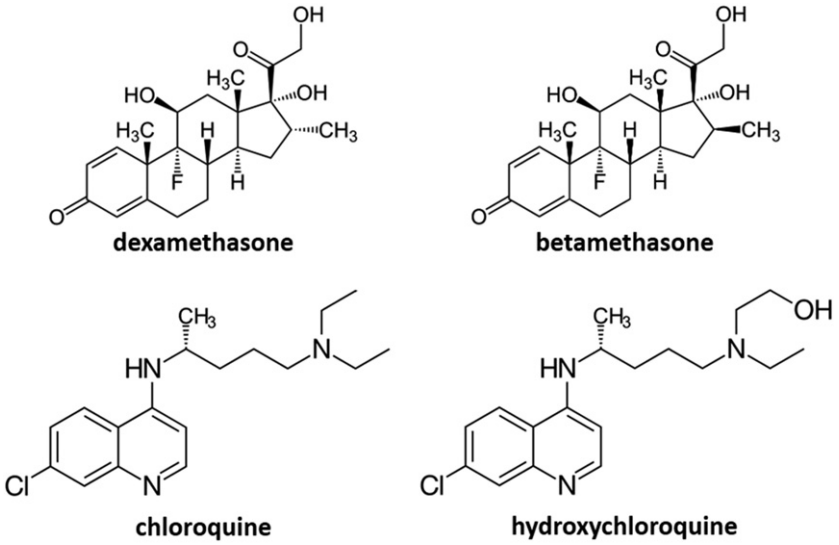

Figure 1. Top: 2D structures of dexamethasone (left) and betamethasone (right). Bottom: 2D structures of chloroquine (left) and hydroxychloroquine (right).

molecular docking calculations using the 6w63 crystal structure of Mpro. Molecular coupling allows us obtaining different possible ligand–receptor combinations, interaction diagrams, as well as determining hydrogen bonds, and the scores. In addition, we have calculated binding energies for the ligands-targets complexes through a molecular mechanics-generalized Born and surface area (MM-GBSA) procedure. Our main goal is to compare the inhibition mechanism of dexamethasone and betamethasone against potential targets of SARS-CoV-2, as well as evaluating any difference in their docking mechanism with those of chloroquine and hydroxychloroquine. We hope that the present study sheds light on the understanding of the interactions that take place between potential drugs and the main SARS-CoV-2 protease, facilitates the design of inhibitors of the activity of this enzyme and, ultimately, it contributes to the advance toward a possible treatment of the disease caused by SARS-CoV-2.

2. Computational methods

Preliminarily, we carried out a conformational search by molecular mechanics using the AMBER force field implemented in the Maestro 12.5 program [22]. Subsequently, the structures of the most stable conformers of dexamethasone, betamethasone, chloroquine, and hydroxychloroquine molecules were optimized in the framework of the density functional theory (DFT) employing the B3LYP exchange–correlation functional. It includes the Becke three-parameter exchange functional [23] and the Lee–Yang–Parr correlation functional [24]. In these quantum mechanics calculations we have used Pople double-zeta 6-31G basis set [25].

At the respective optimized geometries, harmonic vibrational frequencies were calculated to apply zero-point-energy corrections to the electronic energy. Vibrational calculations also allow us to classify the structures as true minima (all of the frequencies are real) or transition state structures (one of the frequencies, and just one, is imaginary).

All quantum mechanical calculations were carried out with the Gaussian 16 program package [26].

The molecular docking approach was used to model the interaction, at atomic level, between dexamethasone, betamethasone, chloroquine and hydroxychloroquine (ligands) and the 6w63 Mpro structure reported in the protein data bank (PDB) [27]. This allows us to characterize the behavior of the ligands in the binding site of the target Mpro structure. The docking process involves two main steps: prediction of the ligands conformations as well as its position and orientation within these sites (usually referred to as pose) and assessment of the binding affinity. These two steps are related to sampling methods and scoring schemes, respectively [12]. The computational analysis was carried out using Maestro v12.5 [22] implemented in the Schrödinger software. It includes packages, ligand preparation, protein preparation wizard [28], Glide XP [29–31], grid-based ligand docking with extra precision and MMGBSA calculations for binding free energy predictions.

3. Results and discussion

3.1. Structure and reactivity parameters

In this section, we report a conformational study of dexamethasone, betamethasone, chloroquine and hydroxychloroquine to ascertain the most stable geometry of each drug. In addition, for the most stable conformer we provide global and local reactivity indices.

Most drugs show structural polymorphism and, firstly, it is necessary to find the most thermodynamically stable structure. In this regard, a molecular mechanics conformational search using the AMBER force field, was carried out. From this search, we selected low energy conformers within a range of 30 kJ mol^{-1}. These structures were subsequently reoptimized

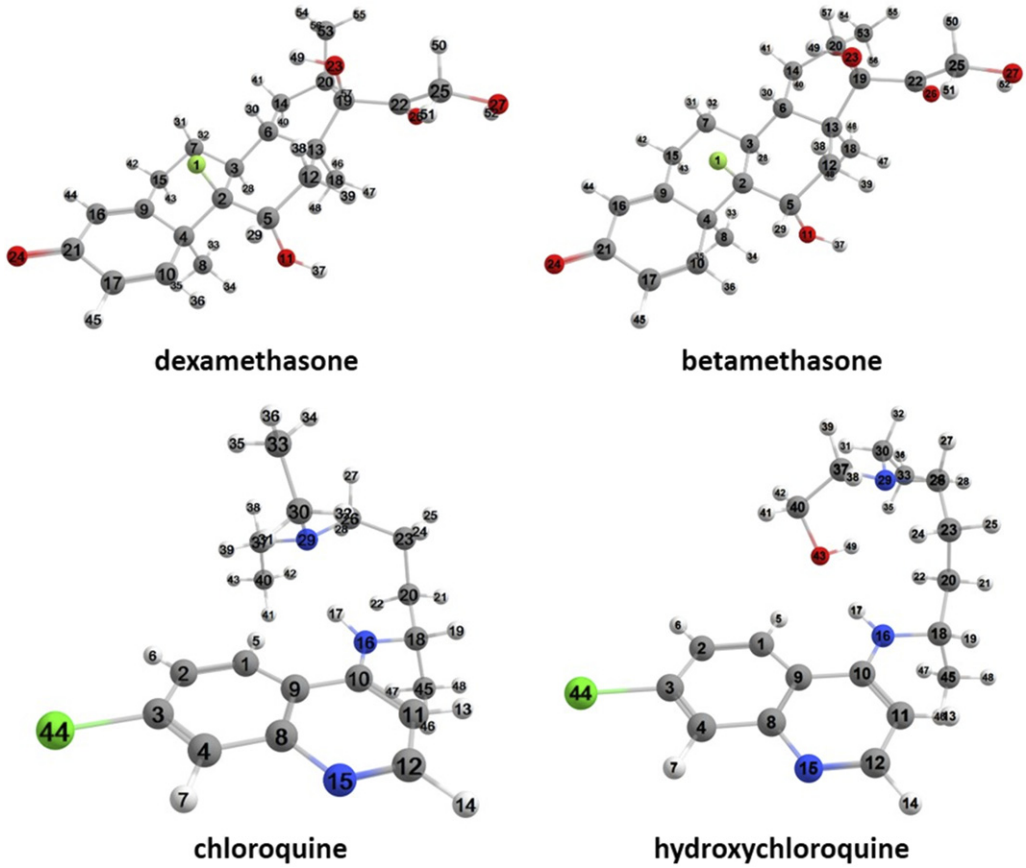

Figure 2. Optimized structures of the most stable structures of dexamethasone (top, left) and betamethasone (top, right), chloroquine (bottom, left) and hydroxychloroquine (bottom, right) at B3LYP/6-31G level. The colors of the various atoms within the molecules follow the standard CPK rules: white for hydrogen, grey for carbon, red for oxygen, blue for nitrogen, and green for chlorine (dark) or fluorine (light).

at B3LYP/6-31G level. In figure 2 we show the B3LYP/6-31G optimized structures for the most stable conformers of dexamethasone, betamethasone, chloroquine and hydroxychloroquine. The coordinates of the optimized most stable structure for each drug are given in tables 1–4 of the supplementary material (https://stacks.iop.org/JPCM/34/295201/mmedia).

To obtain the spectroscopic signatures of dexamethasone, betamethasone, chloroquine and hydroxychloroquine, a vibrational analysis has been performed. The theoretically predicted IR spectra of the lowest energy conformers computed at the B3LYP/6-31G level are shown in figure 3.

As expected, the two IR spectra of dexamethasone and betamethasone are very similar, as they are stereoisomers, the two molecules differing only in the spatial configuration of the methyl group at position C(20). Several characteristic regions can be identified: there is a high IR activity in the 200–300 cm^{-1} region due to the several CH_3 torsions. The high intensity bands observed in the 1600 cm^{-1}–1800 cm^{-1} region correspond to the carbonyl and aromatic C=C stretching modes. Several peaks are present around the 3000 cm^{-1} region due to the C–H stretching modes. Finally, the O–H stretching vibrations of the hydroxyl group were found in the 3500 cm^{-1}–3650 cm^{-1} region. Regarding chloroquine and hydroxychloroquine, there is a prominent peak around 1600 cm^{-1} due to the N–H bending mode. Additionally, for hydroxychloroquine there is sharp peak at c.a. 3600 cm^{-1} due to the free N–H stretching mode. Interestingly, this mode is red-shifted to 3400 cm^{-1} in chloroquine due to the intramolecular N–H•••N hydrogen bond interaction. Finally, the OH stretching mode in hydroxychloroquine appears at 3500 cm^{-1}, which is red-shifted with respect to the typical value of a free OH stretching mode due to the N–H•••O–H hydrogen bond interaction. In fact, the calculations for this stretching mode suggest that there is some coupling between both functional groups. This information shall be useful to better understand the shape of the aforementioned drugs in the isolation conditions of the gas phase, as well as to conclusively unveil their conformational panorama. Moreover, the spectroscopic parameters relevant to rotational spectroscopy (i.e., rotational constants and dipole moment components) are listed in table 5 of the supplementary material.

For the most stable conformers of each structure, we have computed global and local reactivity descriptors. Global reactivity indices, such as chemical hardness, chemical potential and electrophilicity, can be used for rationalizing and predicting some aspects of chemical bonding and reaction mechanisms, whereas local parameters, such as Fukui functions, can give information about site selectivity in a molecule.

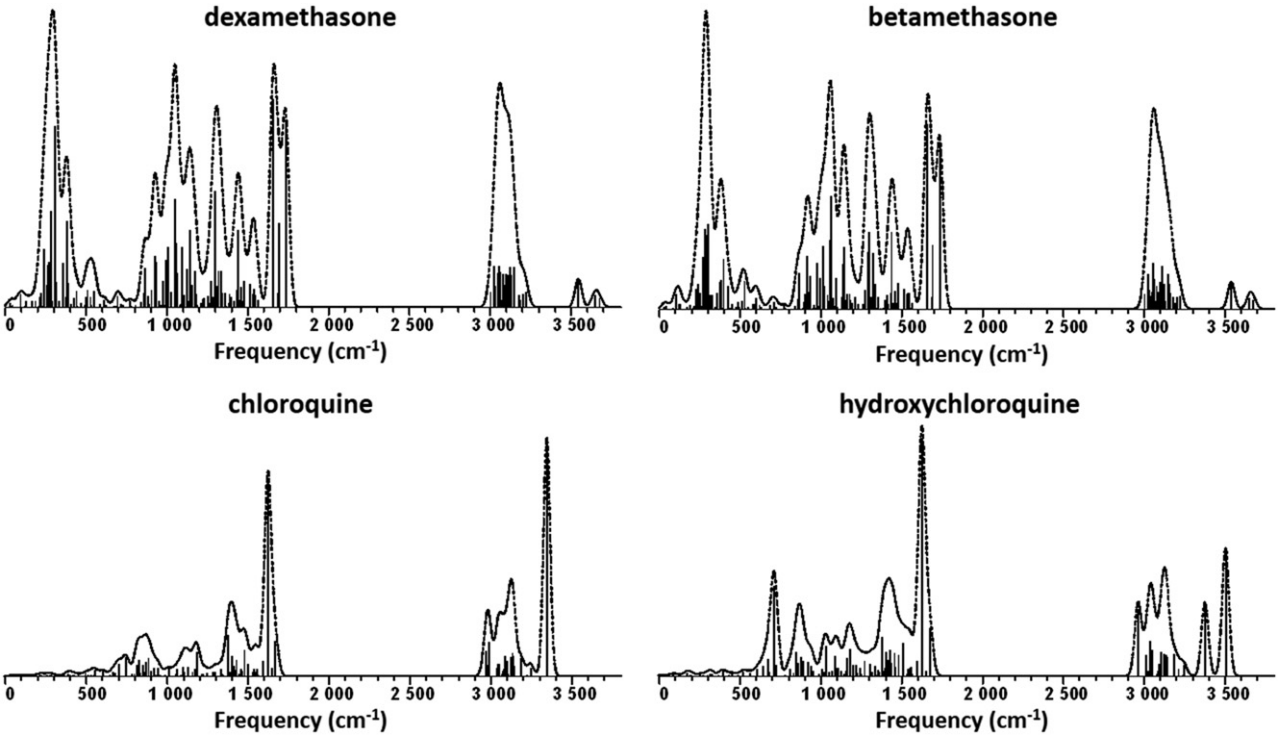

Figure 3. Predicted IR spectra for the optimized structures of dexamethasone (top, left), betamethasone (top, right), chloroquine (bottom, left) and hydroxychloroquine (bottom, right) at B3LYP/6-31G level.

Table 1. B3LYP/6-31G global reactivity indices (in eV) for dexamethasone, betamethasone, chloroquine and hydroxychloroquine.

	Dexamethasone	Betamethasone	Chloroquine	Hydroxychloroquine
I (Vert)	8.18	8.16	6.98	6.91
A (Vert)	−0.22	−0.22	0.57	0.78
I (Adiab)	7.91	7.94	6.79	6.71
A (Adiab)	−0.50	−0.50	0.19	0.32
μ (eV)	−3.71	−3.72	−3.49	−3.52
η (eV)	4.21	4.22	3.30	3.20
σ (eV)	0.24	0.24	0.30	0.31
ω (eV)	3.26	3.28	3.69	3.87

Ionization energies (I) and electron affinities (A) were computed from separated optimizations of the neutral and charged systems including zero-point energy corrections. The chemical potential, (μ), allows to predict whether a change in substance happens voluntarily or not. It is defined as the first order partial derivative of the total energy (E) of the system with respect to the number of electrons (N) at constant external potential (V) and can be determined in terms of the ionization potential I and electron affinity A

$$\mu = \left(\frac{\partial E}{\partial N}\right)_V = \frac{1}{2}(I + A). \tag{1}$$

The terms hardness and softness are generally used to predict the behavior of a molecule and how it reacts with others. Chemical hardness is defined as the resistance of the electron distribution to be disturbed by a small perturbation. This term provides an idea of the stability and reactivity of the system. The global hardness (η) property as described by Parr and Pearson [32] can be expressed either as the first order derivative of the chemical potential or as the second order partial derivative of the total energy of the system with respect to the number of electrons at constant potential:

$$\eta = \left(\frac{\partial \mu}{\partial N}\right)_V = \left(\frac{\partial^2 E}{\partial N^2}\right)_V = \frac{1}{2}(I - A). \tag{2}$$

The inverse of the hardness is denoted as the global softness (σ)

$$\sigma = \frac{1}{\eta}. \tag{3}$$

Finally, the global electrophilicity index (ω) indicates the propensity of a molecule to accept electrons and is calculated

in terms of chemical potential and hardness

$$\omega = \frac{\mu^2}{\eta}. \tag{4}$$

In table 1, we report the global reactivity parameters for dexamethasone, betamethasone, chloroquine and hydroxychloroquine computed at the B3LYP/6-31G level.

As we can see from table 1, both dexamethasone and betamethasone present similar global reactivity parameters. The ionization energy for both molecules is higher than 7.9 eV. This value is equivalent to the wavelength of ∼157 nm corresponding to the far ultraviolet; therefore, these molecules will be stable to visible light. The ionization energy of chloroquine and hydroxychloroquine is ∼6.7 eV, considerably lower than that of dexamethasone and betamethasone, but large enough to be stable under visible light.

The chemical potential for dexamethasone, betamethasone, chloroquine and hydroxychloroquine has a negative value, which indicates that the four molecules could be easily formed and therefore they have a very low tendency to dissociate. Therefore, it can be concluded that they are stable molecules against dissociation.

The difference in energies between the HOMO and LUMO orbitals determines the reactivity and conformational change in many systems. A large difference indicates that the molecule is hard, which is related to the stability of the molecule. The four molecules have a very similar and high chemical potential (∼3.5–3.7 eV). On the other hand, despite that the four molecules have a high hardness, the values of dexamethasone and betamethasone (4.2 eV) are higher than those of chloroquine and hydroxychloroquine (∼3.3 eV). Thus, there is not a large difference in their electrophilicity index.

The above parameters indicate the global reactivity of the molecule, but they do not give information about the reactivity of specific points of a large molecule, such as active sites within a protein. To shed light on the matter, the Fukui functions were computed.

The Fukui function or Frontier function [33, 34] is one of the most used local reactivity parameters. It describes the variation of the electron density after adding or removing electrons and is defined as the derivative of the electron density $\rho(r)$ with respect to the number of electrons N of the system (at constant external potential or molecular geometry)

$$f(r) = \left(\frac{\partial \rho(r)}{\partial N}\right)_v. \tag{5}$$

Due to the discontinuity of the electron density with respect to the total number of electrons, finite difference approximation leads to three Fukui functions governing nucleophilic, electrophilic, and neutral attack. The Fukui function for the addition of an electron to a molecule can be written as:

$$f^+(r) = \rho_{N+1}(r) - \rho_N(r). \tag{6}$$

Equally, the Fukui function for the removal of an electron is:

$$f^-(r) = \rho_N(r) - \rho_{N-1}(r). \tag{7}$$

And the Fukui function for neutral (or radical) attack can be expressed as:

$$f^0(r) = \frac{1}{2}(\rho_{N+1}(r) - \rho_{N-1}(r)). \tag{8}$$

In figure 1 of the supplementary material, we provide figures displaying the Fukui functions for dexamethasone, betamethasone, chloroquine and hydroxychloroquine obtained at the B3LYP/6-31G level.

The Fukui functions can be used to describe local chemical reactivity. This can be defined per atom by using the condensed Fukui function. The condensed Fukui functions for an atom k in a molecule with N electrons can be expressed in terms of charges (q_k) in the neutral (N electrons), cationic ($N-1$ electrons) or anionic ($N+1$ electrons) systems.

The condensed-to-atoms Fukui function which governs nucleophilic attack, f_k^+, electrophilic attack, f_k^-, and homolytic attack f_k^0, can be written, respectively, as:

$$f_k^+ = q_k(N+1) - q_k(N) \tag{9}$$

$$f_k^- = q_k(N) - q_k(N-1) \tag{10}$$

$$f_k^0 = \frac{1}{2}[q_k(N+1) - q_k(N-1)]. \tag{11}$$

The calculation of condensed Fukui functions requires the use of atomic charges. There are several ways to partition the atomic charges. Unlike electron densities, atomic charges are not a quantum-mechanical observable. Atomic charges can be computed in the framework of different population analysis schemes being the most used either Mulliken population analysis (MPA) [35] or natural population analysis [36].

For the calculation of condensed Fukui functions we have used MPA and NBO individual charges computed at the B3LYP/6-31G level. The population analysis on the cationic and anionic systems was performed at the same equilibrium geometry as the neutral counterpart to avoid system relax and thus loosing of information on the polarization of the electron density upon the change in number of electrons.

In tables 6–9 of the supplementary material we give the Fukui indices for dexamethasone and betamethasone obtained from MPA and NBO charges. For dexamethasone and betamethasone the f_k^+ function obtained from NBO charges (tables 6 and 8 of the supplementary material, respectively) show the highest value in the in the carbon atom C(22) which corresponds to the carbonyl group of the side chain, indicating the possible site for nucleophilic attack. Regarding electrophilic attack, the oxygen atom, O(24), which is double bonded to a carbon atom C(21) and is placed in the six-member ring, has the highest f_k^-. This fact indicates that it is the preferred site for electrophilic attack as well as for protonation. This oxygen atom also shows the highest value of f_k^0 and will be the preferred site for a homolytic attack. A somewhat different picture is obtained when the condensed Fukui functions are obtained from Mulliken charges. From the values reported in tables 7 and 9 of the supplementary material, it is seen that the oxygen atom of the six-member ring of both dexamethasone and betamethasone, O(24), has the highest

Table 2. Properties of the pockets for the 6w63 structure.

Pocket	Volume (Å^3)	SiteScore	DScore
1	307.328	1.070	1.152
2	181.104	0.872	0.900
3	292.326	0.898	0.799
4	113.876	0.622	0.568
5	111.818	0.625	0.548

f_k^+ f_k^- and f_k^0 values indicating the possible site for nucleophilic, electrophilic and neutral attack. In the basis of the Mulliken charges, the reactivity order for the electrophilic attack is O(24) > C(22).The Fukui indices of chloroquine and hydroxychloroquine are collected in tables 10–13 of the supplementary material. For condensed Fukui functions obtained from NBO charges (tables 10 and 12 of the supplementary material) the relevant parameters are identical for both molecules: on the one hand, the aromatic carbon atoms C(1), C(4) and C(10), the latter also bonded to the amino group, show the highest f_k^+ value, indicating the possible sites for nucleophilic attack. On the other hand, the aromatic carbon C(11) and the nitrogen N(15) in the same aromatic ring, as well as the nitrogen N(16) next to the aromatic ring, followed by the chlorine atom, have the highest f_k^- indicating that this sites are preferable for an electrophilic attack and the most preferred site for protonation. This oxygen atom also shows the highest value of f_k^0 and will be the preferred site for a homolytic attack. When Mulliken charges are used in the calculation of condensed Fukui functions of chloroquine and hydroxychloroquine (tables 11 and 13 of the supplementary material), the predicted site for nucleophilic, electrophilic and homolytic attack is the chlorine atom.

If one compares the highest f_k^+, f_k^- and f_k^0 values obtained from the NBO charges it is observed that, electrophilic attack has higher reactivity in comparison with the nucleophilic and the homolytic attack. However, when the Mulliken charges are used the nucleophilic attack has higher reactivity than its electrophilic and homolytic counterparts.

It should be noted that the Fukui functions depicted in figure 1 of the supplementary material are consistent with the trends found in the condensed Fukui functions obtained from NBO charges. Some authors have pointed out the failure of the MPA charges to reproduce reactivity sequences [37]. This may be due to the fact that Fukui function describes the soft–soft interactions, whereas the molecular electrostatic potential describes the hard–hard interactions as suggested by Langenaeker *et al* [38].

3.2. Molecular docking studies

Several studies suggested that the interaction between a ligand and Mpro can inhibit the activity of the main protease of SARS-COV-2 [39]. Concretely, recent researches have demonstrated that, dexamethasone could bind to the viral and host receptors as a potential drug candidate for COVID-19 [8, 9]. To evaluate the antiviral activity of different drugs, we have performed a molecular docking analysis against the main protease of SARS-COV-2 Mpro. In this part, our main goal is to test the capacity of several drugs as coronavirus inhibitors and to evaluate their docking at the binding sites of an x-ray Mpro structure. For this purpose, we have selected the 3D crystal structures of this enzyme from PDB of the Structural Bioinformatics Research Laboratory (RCSB) with PDB IDs 6w63. This protein corresponds to SARS-CoV-2 main protease bonded to a potent broad-spectrum non-covalent inhibitor X77.

In a first stage, the X77 cocrystallized ligand was docked into the binding pocket of SARS-CoV-2 main protease to validate the molecular docking procedure. After docking, all poses led to a similar disposition of the 6w63 structure.

Prior to be used as receptors for molecular docking, the 6w63 structure needs to be processed. With this aim, the protein preparation module [28] in Schrödinger was used. The protein preparation wizard includes addition of hydrogen atoms, elimination of solvent molecules (H_2O and DMSO) that are not involved in ligand binding, correction of specific residues or, in the case of the 6w63 structure the preparation process requires to remove the X77 ligand. In this stage, structures were optimized and minimized (hydrogen bonds) using the OLPS2005 field force. During the protein preparation process, we selected a pH of 7.0 to simulate the conditions of the blood in the human body (ranging between 7.35 to 7.45). The different processes of preparation, optimization, minimization and optimization plus minimization structures are relevant to analyze their influence in the final properties emerging from the molecular docking. In this regard, we have computed the root mean square value corresponding to the comparison between pairs of structures obtained after the application of the processes above indicated. We found the optimization as the most relevant step in the protein process. This is mainly because the optimization of hydrogen bonds and bridges modifies the arrangement of the atoms in the structures.

The importance of the two catalytic residues His41 and Cys145 for the design inhibitors against SARS-CoV-2 Mpro has been recently described [5]. In this regard, we use the SiteMap module in Schrödinger to visualize and generate information of binding sites (pockets). A SiteMap calculation begins with an initial search stage that determines one or more regions on or near the protein surface, called sites, that may be suitable for binding of a ligand to the receptor. The search uses a grid of points, called site points, to locate the sites. In the second stage, contour (site) maps are generated, producing hydrophobic and hydrophilic maps which are further divided into donor, acceptor, and metal-binding regions. The evaluation stage assesses each site by calculating various properties. The most important property generated by SiteMap is an overall SiteScore, which has proven to be effective at identifying known binding sites. Other properties characterize the binding site in terms of the size of the site, the degrees of enclosure by the protein and exposure to solvent, the tightness with which the site points interact with the receptor, the hydrophobic and hydrophilic character of the site and the balance between them, and, finally, the degree to which a ligand might donate or accept hydrogen bonds.

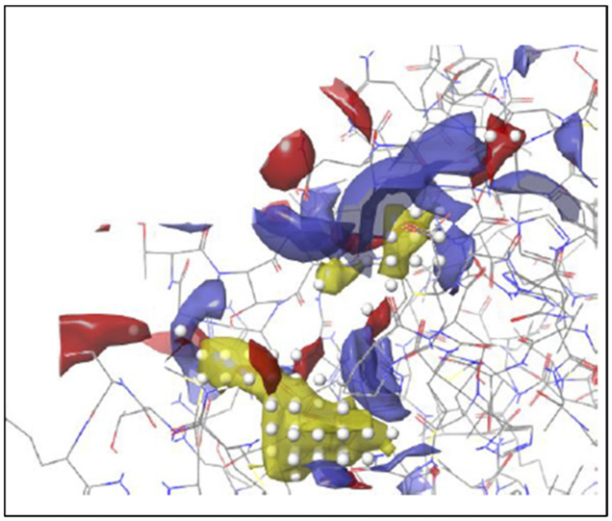

Figure 4. Selected 6w63 pocket. The hydrophobic map is colored in yellow mesh, the hydrophilic map in green mesh, the hydrogen-bond donor map in blue mesh, the hydrogen-bond acceptor map in red mesh, the metal-binding map in pink mesh, and the surface map in gray surface with a 50% transparency.

Table 3. Docking results for X77, dexamethasone, betamethasone, chloroquine and hydroxychloroquine and the energy of interaction with the active site of the 6w63 receptor. Hbond accounts for hydrogen bond, while vdW stands for van der Waals. All the Gibbs free energy values are given in kcal mol^{-1}.

Ligand	XPScore	ΔG	ΔG_{Hbond}	ΔG_{vdW}
X77	−5.00	−104.90	−1.09	−59.52
Dexamethasone	−5.48	−83.91	−0.46	−40.35
Betamethasone	−5.06	−81.85	−0.57	−38.84
Chloroquine	−4.89	−71.55	−0.01	−40.84
Hydroxychloroquine	−5.32	−78.77	−0.26	−38.41

For the 6w63 structure, the SiteMap calculation leads to five active sites or pockets in which docking can occur. In table 2 we report information of the volume, SiteScore and the Dscore of the different pockets.

The SiteScore [40] allows us to identify and compare the binding sites. It is determined taking into account the number of possible sites of link in the pocket, the ease of accessing to the site of interest and the hydrophilic character of the pocket. For non-charged pockets, it is more convenient to use the drug-ability score function (DScore) [40] which takes into account the hydrophilic character of the pocket. The DScore function should be greater than 0.8 for an effective docking.

The pocket 1 in the 6w63 structure has the highest values for volume, SiteScore and DScore parameters, and has inside the, in principle, relevant amino acids (His41, Cys143, Gly145) for docking. Thus, pocket 1, depicted in figure 4, was selected for coupling to the ligand.

Once the pockets are selected, a grid needs to be generated to perform the molecular docking. The grid was focused on the amino acid serine 46 (Ser46) which is found in the center of a 10 Å side cube. For the analysis of the interaction of the protein with the ligand, the Glide approach was used [29, 31]. This methodology allows an exhaustive search for the possible positions and orientations of the ligand in the pocket. Firstly, a ligand conformational search should be performed using the same level that was applied in the protein (OPLS2005). Subsequently, these ligands will be inserted into the generated pocket, using molecular mechanics which is refined using the Monte Carlo procedure to finally obtain the last bonding data, denoted as GlidScore. The GlidScore allows the determination of the Gibbs free energy of the protein–ligand bond as sum of different contributions that accounts for lipophilic, hydrophobic, metal–ligand interaction, rotation of bonds, Coulomb contribution, Van der Waals forces and solvation effects. In this work, the extra precision Glide approach has been used (Glide XP). The extra precision Glide methodology performs the calculation of the binding energy as described above but introduces a new concept: the Glide XP score (XPscore) function that allows to quantify and order the ability of ligands to bind to a specific receptor conformation. To obtain the XP score function, some contributions such as the displacement of water from the active site by the ligand in the hydrophobic regions, the interaction due to the bridges between the protein and the ligand, as well as other electrostatic attractions, such as salt bridges, solvation effects, steric effects due to restrictions in the binding between the protein and the ligand and metal–ligand interactions are considered. The inclusion of these terms allows a score to be given to the link between the receptor and the ligand and, in this way, establish a ranking among all the docking possibilities that find the program. Unlike link energy, the XP GlideScore takes into account interactions that can be detrimental to the bond, encompassed within a penalty parameter.

In table 3 we report the docking scores and the Gibbs binding energy of dexamethasone, betamethasone, chloroquine and hydroxychloroquine with the active site of the 6w63 receptor. The docking results for the X77 cocrystallized ligand of 6w63 are also shown for comparison. As expected, the cocrystallized ligand X77 has the largest Gibbs binding energy (−104.9 kcal mol^{-1}). Among potential inhibitors, dexamethasone exhibits the highest affinity for the 6w63 target with a binding Gibbs free energy of −83.91 kcal mol^{-1}. In addition, the 6w63 receptor complexed with dexamethasone showed the largest XPScore (−5.48).

Dexamethasone was predicted to be preferable for binding to the protein receptor than its enantiomeric form betamethasone, as well as the other two ligands. Table 4 shows that the binding Gibbs free energies for dexamethasone and betamethasone and the 6w63 structure are very similar (∼−83 kcal mol^{-1}), but higher than that of hydroxychloroquine (−78.77 kcal mol^{-1}) and considerably larger than chloroquine (−71.55 kcal mol^{-1}), the latter displaying the lowest affinity for the protein. The examination, in detail, of docking calculations indicates that 6w63 Mpro shows high Van der Waal contributions for the four drugs (∼−41 kcal mol^{-1}). The most important aspect comes from the differences in the hydrogen-bond contribution: for the docking between 6W63 and dexamethasone a contribution of −0.57 kcal mol^{-1} is predicted, followed by betamethasone with a value

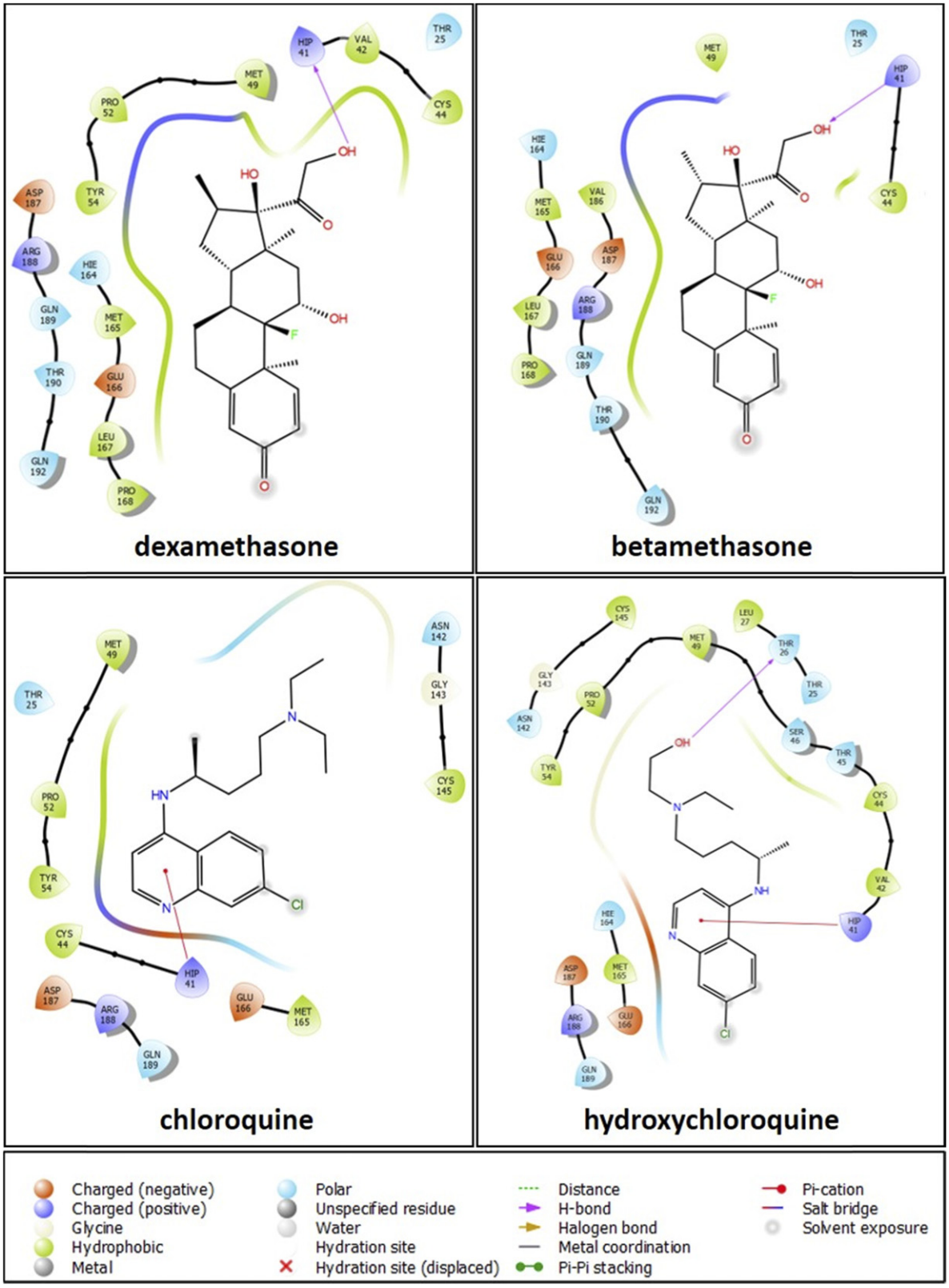

Figure 5. 2D visual representation of the interactions of dexamethasone (top left), betamethasone (top right), chloroquine (bottom left) or hydroxychloroquine (bottom right) within the 6w63' binding pocket.

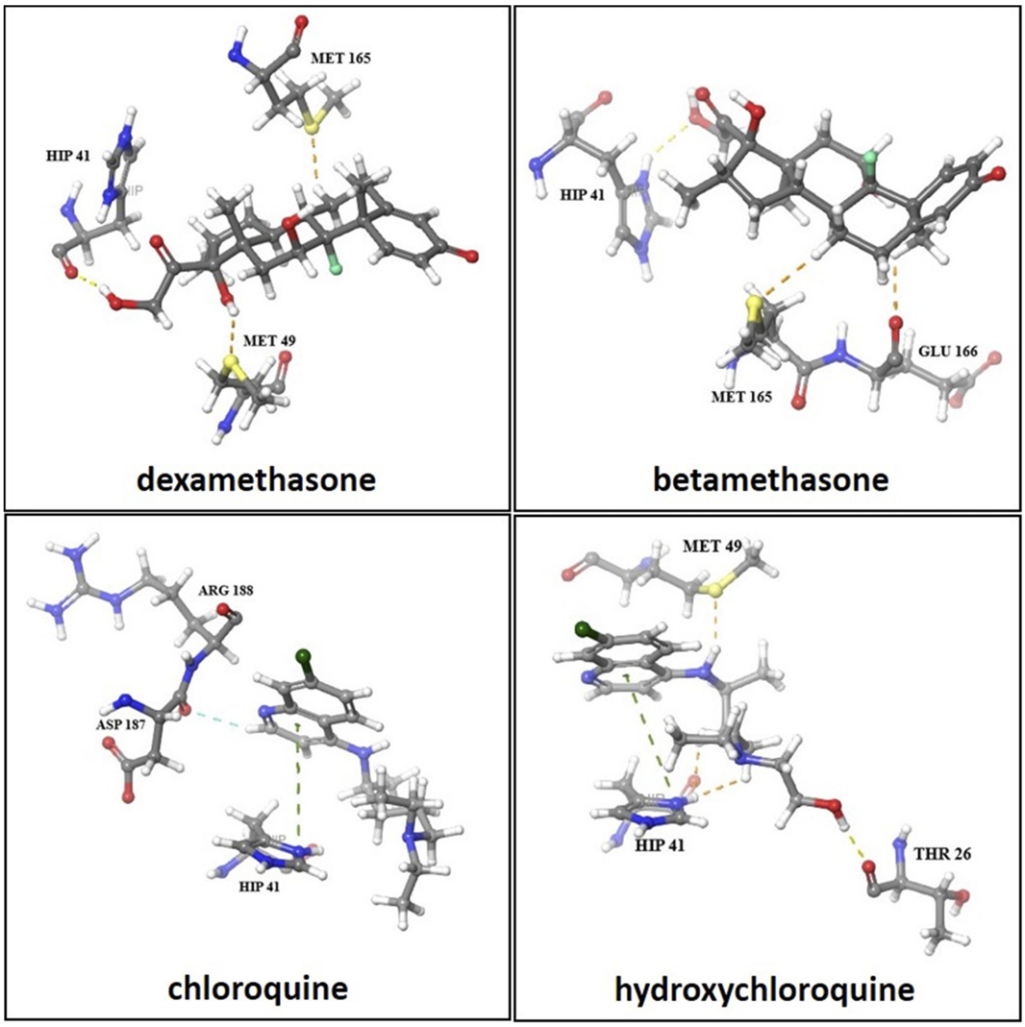

Figure 6. Hydrogen-bond interactions (dotted lines) between the 6w63 structure and either dexamethasone (top left), betamethasone (top right), chloroquine (bottom left) or hydroxychloroquine (bottom right).

of -0.46 kcal mol^{-1}. Interestingly, hydroxychloroquine has half the value, with a stabilization of -0.26 kcal mol^{-1} due to the hydrogen bonds, and chloroquine has a non-existent hydrogen bond contribution. The high inhibition activity of dexamethasone toward the 6w63 protein could be justified by these two strong interactions. In a recent molecular dynamic study [6] was also concluded that dexamethasone was 1.5 times more effective than umifenovir in binding to SARS-CoV-2 Mpro.

The 2D docking pictures of the interactions of the four ligands against those relevant amino acids of the 6w63 target are mapped in figure 5, while figure 6 shows the main molecular interactions between Mpro and the four ligands. We noted that different hydrogen bonds have been established between the protein and each ligand. For dexamethasone, there is a relatively strong O–H•••O=C hydrogen bond between the hydroxyl group in its side chain and the carbonyl oxygen of histidine 41 (Hip41) with a distance of 1.97 Å. Interestingly, in betamethasone this amino acid is also predicted to be critical in the docking process, and there is a N–H•••O–H hydrogen bond formed between the amino group of histidine 41 (Hip41) and the hydroxyl group in the side chain of betamethasone at a distance of 2.28 Å. As it can be seen in figure 6, we also found an OH•••S interaction between the hydroxyl group of dexamethasone and the sulfur atom of methionine 49 (Met49) with a bond distance of 2.38 Å. In the case of betamethasone, a C–H•••O=C interaction between the methyl group of betamethasone and the carbonyl group of glutamine 166 (Glu166) with a bond distance of 2.38 Å is also found. Additional stability comes from the weaker interactions between the sulfur atom of methionine 165 (Met165) and a C–H group of both dexamethasone and betamethasone with bond distances of 2.61 Å and 2.60 Å, respectively.

Regarding chloroquine, there is a C=O•••H–C interaction between the carbonyl group of asparagine 187 (Asn187) and the aromatic methylene at a bond distance of 2.36 Å. A N–H•••π interaction between the amino group of histidine 41 (Hip41) and the aromatic ring of chloroquine at a distance of 4.61 Å further stabilizes the docking between them. For hydroxychloroquine, its docking with the 6w63 protein is mainly stabilized through an O–H•••O=C hydrogen bond between the hydroxyl group of hydroxychloroquine and the carbonyl group of threonine 26 (Thr26) at a bond distance of

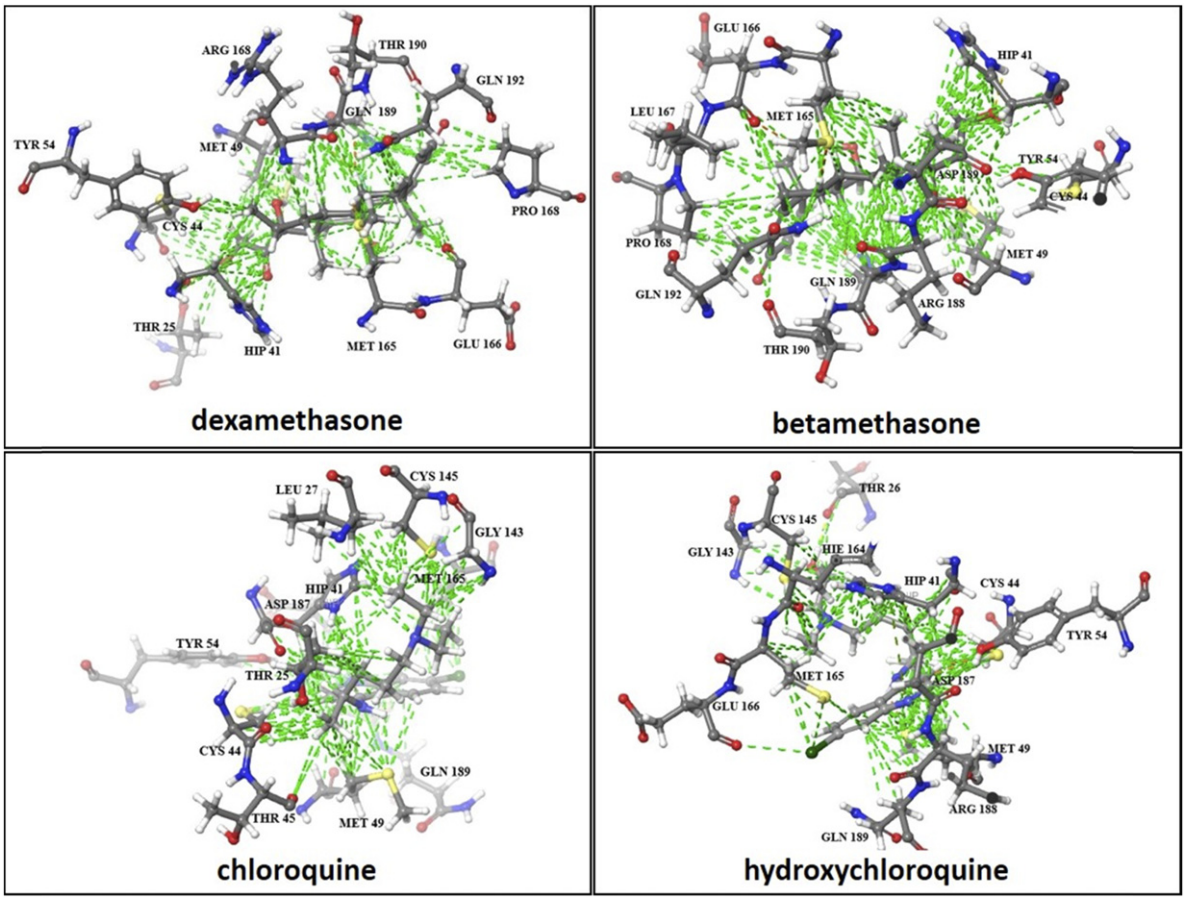

Figure 7. Van der Waals interactions (in green dotted lines) between the 6w63 structure and either dexamethasone (top left), betamethasone (top right), chloroquine (bottom left) or hydroxychloroquine (bottom right).

1.92 Å. Similar to chloroquine, there is an N–H•••π interaction between the amino group of histidine 41 (Hip41) and the aromatic ring of hydroxychloroquine with a distance of 4.52 Å. Finally, we also found weak interactions between the amino group of hydroxychloroquine and the sulfur atom of a methionine 49 amino acid (Met49) at a distance of 2.27 Å.

In addition to all the interactions described above, figure 7 shows that the ligands are linked to the protein through other interactions such as π-alkyl, π-donor, Van der Waals, dispersive forces,.... These interactions confer further overall stability to the complex.

As an additional remark we note that for both dexamethasone and betamethasone, the oxygen O(24) of the carbonyl group, as well as its adjacent aromatic ring, are exposed to the solvent, thus being able to undergo interaction. For chloroquine and hydroxychloroquine, the same is true, in these cases the chlorine atom is exposed to the solvent instead.

3.3. Effectiveness of the potential drugs against COVID-19

Taking the results above into account, we proceed to evaluate the effectiveness of dexamethasone, betamethasone, chloroquine and hydroxychloroquine as potential drug candidates to treat infected people with COVID-19.

The four drugs studied in this work are stable to visible light, as well as being stable against dissociation. This indicates that dexamethasone, betamethasone, chloroquine and hydroxychloroquine can be safely stored under ambient light without further precautions.

There is a large difference in the electrophilicity index of the different drugs (see table 1) with dexamethasone and betamethasone molecules being superior electrophiles. Thus, they show greater propensity to accept electrons and, *a priori*, should be the most efficient ligands in molecular docking.

The docking process is controlled by the difference in Gibbs free energy between the ligands solvated by the extracellular medium and the ligand interacting with the receptor's active site. Therefore, a deep knowledge of the interactions inside the cavity helps to understand the docking process. The results show that all the drugs have a high affinity for the docking process inside the 6w63 pocket. This is particularly true for dexamethasone, which shows the highest affinity with a relatively high binding Gibbs free energy (-83.91 kcal mol^{-1}), as well as the highest XPScore (-5.48). This indicates that, statistically, dexamethasone has a higher chance to interact with the main protease of the SARS-CoV-2 virus MPro. On the other hand, the Gibbs free energy of chloroquine is almost 15 kcal mol^{-1} lower, and thus its docking is less efficient. Furthermore, it has been proposed that histidine 41 (His41) and cysteine 145 (Cys145) are key amino acids to inhibit the SARS-CoV-2 Mpro activity [5, 20]. Despite that we did not find any particular strong interaction in any of the drugs studied

with the cysteine 145 (Cys145) residue, we found that dexamethasone and betamethasone form a relatively strong hydrogen bond with the histidine 41 amino acid (His41). On the other hand, nor chloroquine neither hydroxychloroquine shows a strong interaction with histidine 41 (His41), and their interaction with histidine 41 (His41) is through a weak C–H•••π interaction. Therefore, our results support that histidine 41 (His41) could be key for the docking process. Additionally, dexamethasone shows a high affinity which may be important when interacting with the key enzyme of COVID-19 during its viral replication and transcription process. Interestingly, our modeling is in good agreement with the experimental findings in which dexamethasone has shown a positive effect for treating COVID-19 patients, while it was concluded that chloroquine and hydroxychloroquine are not an effective treatment for COVID-19.

As a final remark, our calculations also showed that the O(24) oxygen atom bound to the C(21) carbon atom in both dexamethasone and betamethasone has the highest f_k^- indicating the site for electrophilic attack, as well as the most preferred site for protonation. Interestingly, we also found that this O(24) oxygen atom is exposed to the solvent during the docking process. Probably this fact reinforces the docking process by stabilizing the molecule, not only inside the cavity, but with the surrounding media too. Furthermore, if the preferred site for protonation would have been any atom of the ligand located within the cavity, it could lead to unexpected consequences. Therefore, we also propose that not only the docking process is important but also the ability to protect the ligand inside the cavity, while conferring stability with the inside and outside of the cavity at the same time, which is intrinsically related to the shape of the molecule.

4. Conclusion

The drugs dexamethasone, betamethasone, chloroquine and hydroxychloroquine have been theoretically characterized using molecular and quantum mechanics and molecular docking methodologies. Their structural and conformational properties have been investigated through molecular mechanics calculations. The lowest energy conformers for each drug have been identified and reoptimized at the B3LYP/6-31G level to provide meaningful spectroscopic parameters that could help in future structural characterizations. DFT was also used to obtain global and local reactivities. No significant differences were found in the global and local reactivity indices of dexamethasone and betamethasone, but their values are considerably larger than those of chloroquine and hydroxychloroquine.

The lower energy conformers for the four ligands were used in a molecular docking study with potential active sites of the 6w63 structure for the SARS-CoV-2 main protease. The results obtained from the docking calculations show that dexamethasone and betamethasone prefer to bind to the 6w63 target sites, particularly for dexamethasone. Concerning the efficiency for molecular docking, we found a higher affinity for dexamethasone with a binding Gibbs free energy of -83.91 kcal mol^{-1}, than for betamethasone with a binding Gibbs free energy of -81.85 kcal mol^{-1}. The affinity of hydroxychloroquine is lower with a binding Gibbs free energy of -78.77 kcal mol^{-1}, and with that of chloroquine being considerably lower with a binding Gibbs free energy of -71.55 kcal mol^{-1}.

We found that the histidine 41 amino acid (His41) is key for the docking process between the protein and dexamethasone or betamethasone, as there is a strong ligand–protein hydrogen bond with this amino acid, while chloroquine and hydroxychloroquine show a weak C–H•••π interaction with histidine 41 (His41).

All in all, our computational study confirms the antiviral activity of dexamethasone against COVID-19.

Acknowledgments

Antonio Largo would like to dedicate this article to the memory of Enrico Clementi. Enrico was his supervisor during a postdoctoral stay at IBM-Kingston and strongly influenced his scientific and academic career, being always an inspiration. He also wants to express his gratitude and affection to Gina Corongiu. The authors thank the financial fundings from Ministerio de Ciencia e Innovación (PID2019-111396GB-I00 and PID2020-117742GB-I00), and Junta de Castilla y León (Grant VA244P20). MSN acknowledges funding from the Spanish 'Ministerio de Ciencia, Innovación y Universidades' under predoctoral FPU Grant (FPU17/02987).

Data availability statement

All data that support the findings of this study are included within the article (and any supplementary files).

ORCID iDs

Miguel Sanz-Novo https://orcid.org/0000-0001-9629-0257
Iker León https://orcid.org/0000-0002-1992-935X
Pilar Redondo https://orcid.org/0000-0001-7876-4818
Antonio Largo https://orcid.org/0000-0003-4959-4850
Carmen Barrientos https://orcid.org/0000-0003-0078-7379

References

[1] Wang L, Wang Y, Ye D and Liu Q 2020 Review of the 2019 novel coronavirus (SARS-CoV-2) based on current evidence *Int. J. Antimicrob. Agents* **55** 105948
[2] Lu R *et al* 2020 Genomic characterisation and epidemiology of 2019 novel coronavirus: implications for virus origins and receptor binding *Lancet* **395** 565–74
[3] Maier H J, Bickerton E and Britton P 2015 *Coronaviruses: Methods and Protocols* vol 1282 (New York: Humana) pp 1–282
[4] Hegyi A and Ziebuhr J 2002 Conservation of substrate specificities among coronavirus main proteases *J. Gen. Virol.* **83** 595–9
[5] Zhang L, Lin D, Sun X, Curth U, Drosten C, Sauerhering L, Becker S, Rox K and Hilgenfeld R 2020 Crystal structure of SARS-CoV-2 main protease provides a basis for design of improved α-ketoamide inhibitors *Science* **368** 409–12
[6] Nayeem S M, Sohail E M, Ridhima G and Reddy M S 2021 Target SARS-CoV-2: computation of binding energies with drugs of dexamethasone/umifenovir by molecular dynamics using OPLS-AA force field *Res. Biomed. Eng.* **38** 117–26

[7] De Wasch K, De Brabander H F, Van De Wiele M, Vercammen J, Courtheyn D and Impens S 2001 Differentiation between dexamethasone and betamethasone in a mixture using multiple mass spectrometry *J. Chromatogr.* A **926** 79–86

[8] Caruso F, Rossi M, Pedersen J Z and Incerpi S 2020 Computational studies reveal mechanism by which quinone derivatives can inhibit SARS-CoV-2. Study of embelin and two therapeutic compounds of interest, methyl prednisolone and dexamethasone *J. Infect. Public Health* **13** 1868–77

[9] Fadaka A O, Sibuyi N R S, Madiehe A M and Meyer M 2020 Computational insight of dexamethasone against potential targets of SARS-CoV-2 *J. Biomol. Struct. Dyn.* **40** 1–11

[10] Chivese T *et al* 2021 Efficacy of chloroquine and hydroxychloroquine in treating COVID-19 infection: a meta-review of systematic reviews and an updated meta-analysis *Travel Med. Infect. Dis.* **43** 102135

[11] Singh B, Ryan H, Kredo T, Chaplin M and Fletcher T 2021 Chloroquine or hydroxychloroquine for prevention and treatment of COVID-19 *Cochrane Database Syst. Rev.* **2** 1–92

[12] Meng X-Y, Zhang H-X, Mezei M and Cui M 2012 Molecular docking: a powerful approach for structure-based drug discovery *Curr. Comput. Aided-Drug Des.* **7** 146–57

[13] Sethi A, Joshi K, Sasikala K and Alvala M 2020 Molecular docking in modern drug discovery: principles and recent applications *Drug Discovery and Development—New Advances* (London: IntechOpen) pp 1–21

[14] Muhammad I A, Muangchoo K, Muhammad A, Ajingi S, Muhammad I Y, Umar I D and Muhammad A B 2020 A computational study to identify potential *Computation* **8** 1–14

[15] Liu Q, Wan J and Wang G 2021 A survey on computational methods in discovering protein inhibitors of SARS-CoV-2 *Brief. Bioinform.* **23** 1–13

[16] Yan F and Gao F 2021 An overview of potential inhibitors targeting non-structural proteins 3 (PLpro and Mac1) and 5 (3CLpro/Mpro) of SARS-CoV-2 *Comput. Struct. Biotechnol. J.* **19** 4868–83

[17] Wu C *et al* 2020 Analysis of therapeutic targets for SARS-CoV-2 and discovery of potential drugs by computational methods *Acta Pharm. Sin.* B **10** 766–88

[18] Shcherbakov D *et al* 2022 Design and evaluation of bispidine-based SARS-CoV-2 main protease inhibitors *ACS Med. Chem. Lett.* **13** 140–7

[19] Zhang C-H *et al* 2021 Potent noncovalent inhibitors of the main protease of SARS-CoV-2 from molecular sculpting of the drug perampanel guided by free energy perturbation calculations *ACS Cent. Sci.* **7** 467–75

[20] Ghosh R, Chakraborty A, Biswas A and Chowdhuri S 2020 Potential therapeutic use of corticosteroids as SARS CoV-2 main protease inhibitors: a computational study *J. Biomol. Struct. Dyn.* **40** 2053–66

[21] Mitjà O *et al* 2021 Hydroxychloroquine for early treatment of adults with mild coronavirus disease 2019: a randomized, controlled trial *Clin. Infect. Dis.* **73** 4073–81

[22] 2021 Schrödinger Release 2022-1: Maestro *(version 12.5)* (New York, NY: Schrödinger LLC)

[23] Becke A D 1993 Density-functional thermochemistry: III. The role of exact exchange *J. Chem. Phys.* **98** 5648–52

[24] Lee C, Yang W and Parr R G 1988 Development of the Colle-Salvetti correlation-energy formula into a functional of the electron density *Phys. Rev.* B **37** 785–9

[25] Pople J A, Schleyer P V, Hehre W J and Radom L 1986 *Ab initio* molecular orbital theory *AB INITIO Molecular Orbital Theory* vol 7 (New York: Wiley) p 30379

[26] Frisch M J *et al* 2016 *Gaussian 16, Revision A.03* https://gaussian.com/citation/

[27] Mesecar A D 2020 RCSB PDB–6W63: structure of COVID-19 main protease bound to potent broad-spectrum non-covalent inhibitor X77 https://rcsb.org/structure/6w63

[28] Madhavi Sastry G, Adzhigirey M, Day T, Annabhimoju R and Sherman W 2013 Protein and ligand preparation: parameters, protocols, and influence on virtual screening enrichments *J. Comput. Aided Mol. Des.* **27** 221–34

[29] Friesner R A *et al* 2004 Glide: a new approach for rapid, accurate docking and scoring: I. Method and assessment of docking accuracy *J. Med. Chem.* **47** 1739–49

[30] Halgren T A, Murphy R B, Friesner R A, Beard H S, Frye L L, Pollard W T and Banks J L 2004 Glide: a new approach for rapid, accurate docking and scoring: II. Enrichment factors in database screening *J. Med. Chem.* **47** 1750–9

[31] Friesner R A, Murphy R B, Repasky M P, Frye L L, Greenwood J R, Halgren T A, Sanschagrin P C and Mainz D T 2006 Extra precision Glide: docking and scoring incorporating a model of hydrophobic enclosure for protein−ligand complexes *J. Med. Chem.* **49** 6177–96

[32] Parr R G and Pearson R G 1983 Absolute hardness: companion parameter to absolute electronegativity *J. Am. Chem. Soc.* **105** 7512–6

[33] Yang W, Parr R G and Pucci R 1984 Electron density, Kohn–Sham Frontier orbitals, and Fukui functions *J. Chem. Phys.* **81** 2862–3

[34] Parr R G and Yang W 1984 *J. Am. Chem. Soc.* **106** 4049–4050

[35] Mulliken R S 1955 Electronic population analysis on LCAO–MO molecular wave functions: I *J. Chem. Phys.* **23** 1833–40

[36] Reed A E, Weinstock R B and Weinhold F 1985 Natural population analysis *J. Chem. Phys.* **83** 735–746

[37] Arulmozhiraja S and Kolandaivel P 1997 Condensed Fukui function: dependency on atomic charges *Mol. Phys.* **90** 55–62

[38] Langenaeker W, Demel K and Geerlings P 1991 Quantum-chemical study of the Fukui function as a reactivity index *J. Mol. Struct. THEOCHEM* **234** 329–42

[39] Abel R *et al* 2020 Computational prediction of potential inhibitors of the main protease of SARS-CoV-2 *Front. Chem.* **8** 1–19

[40] Halgren T A 2009 Identifying and characterizing binding sites and assessing druggability *J. Chem. Inf. Modelling* **49** 377–89